SUM RULES AND EXCLUSIVE PROCESSES IN QCD*

By A. V. Radyushkin

Laboratory of Theoretical Physics, Joint Institute for Nuclear Research, Dubna**

(Received November 10, 1983)

A brief review is given of a new approach to exclusive form factors of the hadrons at moderately large momentum transfers. The basic idea is to fix the parameters of the soft wave functions of the hadrons by QCD sum rules and to incorporate the local quark-hadron duality to calculate the form factors. After comparing the results obtained with experimental data we conclude that the observed power-law behaviour of the hadronic form factors has nothing to do with short distances and scale invariance.

PACS numbers: 12.35.Cn, 12.35.Eq

1. Introduction

The quark counting rules (QCR) [1, 2] are now a part of the high energy physics "folklore". These rules predict, in particular, that a spin-averaged form factor of a hadron constituted by n quarks should behave asymptotically like t^{1-n} (where $t = Q^2 = -q^2$ and q is the momentum transfer). According to Brodsky and Farrar [2] the specific dynamical mechanism responsible for the QCR is the hard rescattering of quarks that constitute the hadrons participating in the high momentum transfer process. The simple parton-like picture proposed in Ref. [2] was justified later within the framework of the perturbative QCD [3, 4]. It was demonstrated, in particular, that in the asymptotic $t \to \infty$ region the QCD-effects produce only a logarithmic violation of the QCR power-law behaviour of the meson and nucleon electromagnetic form factors [3–8].

A very important question, however, is how large should be the momentum transfer to be considered as an asymptotic one? There are attempts to extract the answer to this question from available experimental data. In particular, for the pion the product $Q^2F_\pi(Q^2)$ is practically constant starting from $Q^2 \approx 1$ GeV^2, while for the nucleons the products $Q^4G^N_{E,M}(Q^2)$ are almost constant for Q^2 in the region $Q^2 \gtrsim 2-3$ GeV^2. This fact is usually interpreted (see, e.g., Refs. [4, 6]) that for Q^2 as low as 1 GeV^2 (for the pion)

* Presented at the XXIII Cracow School of Theoretical Physics, Zakopane, May 29—June 12, 1983.

** Address: Joint Institute for Nuclear Research, 10 10 00 Moscow, Head Post Office P.O. Box 79, USSR.

or $2-3$ GeV^2 (for the nucleons) one observes the asymptotic scaling law corresponding to dominance of the hard rescattering diagrams shown in Fig. 1. However, it is not an easy task to justify such an interpretation within the QCD framework.

For the nucleon, for example, the contribution due to diagrams of the type of Fig. 1b is, in a sense, only the third term of the QCD expansion resulting from applying to $G^N(Q^2)$ the standard procedure of separating long- and short-distance contributions (see Fig. 2).

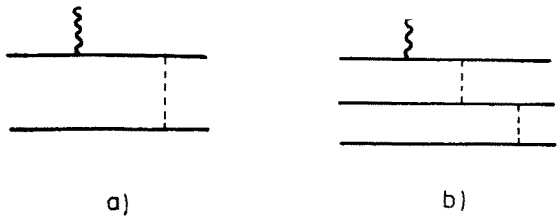

Fig. 1. Diagrams responsible for the large-Q^2 asymptotics of a) pion and b) nucleon form factors

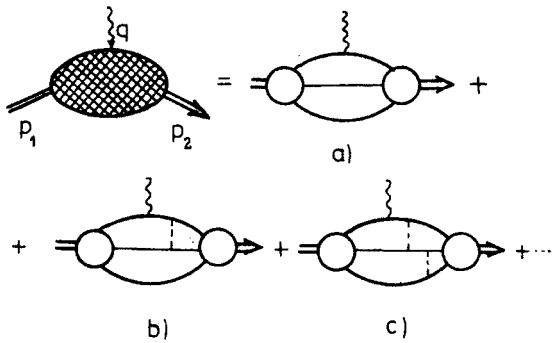

Fig. 2. Structure of factorization for the nucleon form factors. The generalized quark-hadron vertices (including the quark lines adjoint to them) correspond to long distances (small off-shellnesses) while the remaining quark and gluon lines — to short ones, i.e. to the off-shellnesses larger than typical hadronic scale $\lambda^2 = O(1\ \text{GeV}^2)$

To estimate the relative contributions of Figs. 2a–c one should take into account that for $Q^2 = 0$ the main contribution to $G^N(Q^2)$ is given by the simplest diagram 2a. Furthermore, according to the usual "loop counting" the higher order diagrams 2b, c are damped by $\alpha_s(m_N)/\pi \sim 0.1$ and $(\alpha_s(m_N)/\pi)^2 \sim 0.01$ factors, respectively (m_N is the nucleon mass). This means that there should exist a region $Q^2 \lesssim Q^2_{max}$ where the simplest diagram 2a dominates in spite of the fact that in the asymptotic region its contribution vanishes faster than that of Fig. 2c. According to the perturbative estimates (to be justified below) the contribution of Fig. 2a vanishes only like $1/Q^6$, and one should expect that Q^2_{max} is as large as $O((\alpha_s/\pi)^{-2}) \cdot 1$ GeV^2.

To get a more reliable estimate of the contributions of Figs. 2a–c, one should know the soft nucleon wave function. This task cannot, of course, be solved by using the ordinary perturbation theory, since the very existence of hadrons in QCD is largely due to non-perturbative effects.

Among the existing approaches to the analysis of the nonperturbative effects technically most close to the perturbative QCD is the QCD sum rule approach [9, 10]. It was successfully applied earlier to the computation of some essentially nonperturbative hadron characteristics such as masses, leptonic widths, and more recently, electromagnetic form factors of the hadrons at moderate momentum transfers [11–15]. In the present paper a short review of the results [11–12, 14–15] obtained by the author in collaboration with V. A. Nesterenko will be given.

Our main conclusion from these studies is that to describe the existing experimental data on the EM form factors of the pion, proton and neutron it is sufficient to take into account only the simplest (nonperturbative) diagrams that, like Fig. 2a, do not contain any gluon exchanges. This means that, contrary to a widespread belief, the experimental verification of the power law based on the QCR *does not imply* that the main contribution in a given Q^2-region comes from the diagrams involving a short-distance subprocess.

2. *QCD sum rule analysis of the pion EM form factor [11–13]*

The QCD sum rule approach is based on the quark-hadron duality concept, i.e. on the observation that the characteristics of the hadronic spectrum are integrally (i.e., after averaging over an appropriate energy region) close to analogous characteristics computed in perturbation theory for free or not very strong interacting quarks. The nonperturbative effects (that determine, in particular, the widths of the averaging interval) are taken into account by introducing into the theory nonvanishing vacuum averages (condensates) of quark and gluon fields [9].

To analyse the pion form factor within the QCD sum rule approach one should consider the 3-point function

$$T^{\mu}_{\alpha\beta}(p_1, p_2) = i^2 \int d^4x d^4y e^{-ip_1x + ip_2y} \langle 0|\mathrm{T}\{j_\beta(y) J^\mu(0) j^+_\alpha(x)\}|0\rangle \qquad (1)$$

where $J^\mu = \frac{2}{3}\bar{u}\gamma^\mu u - \frac{1}{3}\bar{d}\gamma^\mu d$ is the electromagnetic current and $j_\alpha = \bar{d}\gamma_5\gamma_\alpha u$ is the axial current (our notation corresponds to Fig. 3a). The latter, as it is well-known, has a nonzero projection onto the pion state $|P\rangle$:

$$\langle 0|j_\alpha(0)|P\rangle = if_\pi P_\alpha,$$

where $f_\pi = 132$ MeV is the pion decay constant.

The amplitude $T^{\mu}_{\alpha\beta}(p_1, p_2)$ is the sum of various structures: $P^\mu P^\alpha P^\beta$, $P^\mu P^\alpha q^\beta$, $P^\mu q^2 g^{\alpha\beta}$, etc., where $P = p_1 + p_2$, $q = p_2 - p_1$. The corresponding invariant amplitudes T_i depend on three variables: p_1^2, p_2^2 and q^2. To compare the contributions of these different structures to $T^{\mu}_{\alpha\beta}$ one should specify, of course, the reference frame. In our case (just as in many others) very convenient is the infinite momentum frame (IMF) where $P^\mu \equiv P^\mu_{\|} \to \infty$ while $q^\mu \equiv q^\mu_\perp$ is fixed. The leading IMF structure is clearly $P^\mu P^\alpha P^\beta$ since it does not contain the "small" parameter q. Furthermore, this structure is most close to the structure $P^\alpha P^\beta$ present in the 2-point function $\pi_{\alpha\beta}(P)$ related to the correlator of two axial currents.

Owing to the asymptotic freedom, one may calculate the amplitude $T(p_1^2, p_2^2, Q^2)$ in the deep Euclidean region $p_1^2, p_2^2 \lesssim -1\ \mathrm{GeV}^2$. To extract information about the form factors of physical states, we use the double dispersion relation

$$T(p_1^2, p_2^2, Q^2) = \frac{1}{\pi^2}\int_0^\infty ds_1 \int_0^\infty ds_2 \frac{\varrho(s_1, s_2, Q^2)}{(s_1 - p_1^2)(s_2 - p_2^2)} + (\text{subtraction terms}). \tag{2}$$

The subtraction terms are polynomials in p_1^2 and/or p_2^2. They disappear after one applies to Eq. (2) the SVZ-transformation [9]:

$$B(p^2 \to M^2) = \lim_{\substack{n\to\infty \\ -p^2\to\infty}} \frac{(-p^2)^n}{(n-1)!}\left(\frac{d}{dp^2}\right)^n\Bigg|_{p^2=-nM^2} \tag{3}$$

in p_1^2 and p_2^2. As a result, one obtains from (2):

$$\Phi(M_1^2, M_2^2, Q^2) = \frac{1}{\pi^2}\int_0^\infty \frac{ds_1}{M_1^2}\int_0^\infty \frac{ds_2}{M_2^2}\, e^{-\frac{s_1}{M_1^2}-\frac{s_2}{M_2^2}}\varrho(s_1, s_2, Q^2), \tag{4}$$

where $\Phi \equiv B_1 B_2 T$.

The perturbative contribution to $T(p_1^2, p_2^2, Q^2)$ (corresponding to diagrams of Fig. 3) can also be written in the form of Eq. (2), and $\Phi^{\mathrm{pert}} \equiv B_1 B_2 T^{\mathrm{pert}}$ in the form of Eq. (4). A straightforward calculation gives in the lowest (i.e., zero) order in α_s the following expression for Φ^{pert}:

$$\Phi^{\mathrm{pert}}(M_1^2, M_2^2, Q^2) = \frac{3}{2\pi^2(M_1^2+M_2^2)}\int_0^1 x(1-x)\exp\left\{-\frac{xQ^2}{(1-x)(M_1^2+M_2^2)}\right\}dx. \tag{5}$$

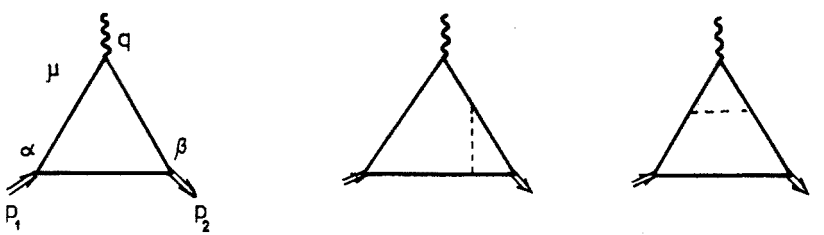

Fig. 3. Diagrams contributing to the perturbative spectral density $\varrho^{\mathrm{pert}}(s_1, s_2, Q^2)$

Note that we neglected in Eq. (5) masses of light quarks u, d ($m_{u,d} \lesssim 10$ MeV). The variable x in Eq. (5) may be interpreted as the fraction of the total pion momentum carried in the IMF by the passive quark.

Using the fact that Eq. (4) has a form of the double Laplace transformation in $1/M_{1,2}^2$, one can extract from Eq. (5) the free-quark (perturbative) spectral density

$$\varrho^{\mathrm{pert}}(s_1, s_2, Q^2) = \tfrac{3}{4} Q^4 \left\{\left(\frac{d}{dQ^2}\right)^2 + \frac{Q^2}{3}\left(\frac{d}{dQ^2}\right)^3\right\}[(s_1+s_2+Q^2)^2 - 4s_1 s_2]^{-1/2}. \tag{6}$$

The physical (or hadron) spectral density $\varrho(s_1, s_2, Q^2)$ differs, of course, from $\varrho^{\text{pert}}(s_1, s_2, Q^2)$. In particular, $\varrho(s_1, s_2, Q^2)$ contains the pion $\delta\delta$-term:

$$\varrho_\pi(s_1, s_2, Q^2) = \pi^2 f_\pi^2 F_\pi(Q^2)\delta(s_1 - m_\pi^2)\delta(s_2 - m_\pi^2) \tag{7}$$

and vanishes everywhere (except the point $s_1 = s_2 = m_\pi^2$) below the 3π-threshold. Only in the region where both s_1, s_2 are sufficiently large, and the resonances are very broad (and overlapping) one may expect that $\varrho \approx \varrho^{\text{pert}}$. This means that $\Phi(M_1^2, M_2^2, Q^2)$ differs also from Eq. (5) calculated for the free quarks. As emphasized in Ref. [9], the difference is largely due to nonperturbative power corrections $(1/M^2)^N$ generated by quark $\langle\bar{q}q\rangle$ and gluon $\langle GG\rangle$ condensates. Taking into account the lowest power corrections (typical diagrams are presented in Fig. 4) we find for $M_1 = M_2 = M$

$$\Phi(M^2, M^2, Q^2) = \Phi^{\text{pert}}(M^2, M^2, Q^2) + \frac{\alpha_s\langle G_{\mu\nu}^a G_{\mu\nu}^a\rangle}{12\pi M^6} + \frac{208\pi\alpha_s}{81 M^8}\langle\bar{q}q\rangle^2\left(1 + \tfrac{2}{13}\frac{Q^2}{M^2}\right). \tag{8}$$

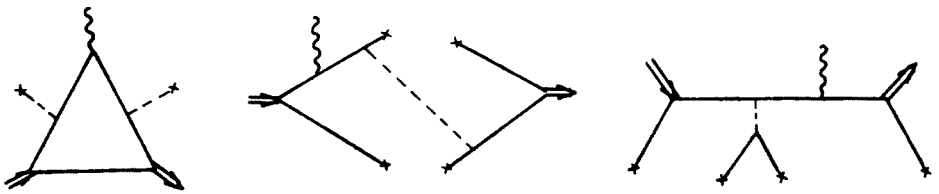

a) b) c)

Fig. 4. Typical diagrams describing the nonperturbative effects proportional to a) $\langle G_{\mu\nu}^a G_{\mu\nu}^a\rangle$ and b, c) $\alpha_s\langle\bar{q}q\rangle^2$

Now, representing the hadronic spectral density $\varrho(s_1, s_2, Q^2)$ as

$$\varrho(s_1, s_2, Q^2) = \varrho_\pi(s_1, s_2, Q^2) + \varrho^{\text{pert}}(s_1, s_2, Q^2)\{1 - \theta(s_1 < s_0)\theta(s_2 < s_0)\} \tag{9}$$

(i.e., assuming that everywhere outside the square defined by $s_1, s_2 < s_0$ the hadronic density coincides with the quark one), equating Eqs. (4) and (8) and taking into account Eqs. (6), (7), (9), we obtain the sum rule that relates the characteristics of the hadronic spectrum (in our case these are $f_\pi^2 F_\pi(Q^2)$ and s_0 — the effective threshold for higher states production; while the pion mass is assumed to have its chiral limit value $m_\pi^2 = 0$) with the quantities calculated theoretically

$$f_\pi^2 F_\pi(Q^2) = \frac{1}{\pi^2}\int_0^{s_0} ds_1 \int_0^{s_0} ds_2 \varrho^{\text{pert}}(s_1, s_2, Q^2) e^{-\frac{s_1+s_2}{M^2}}$$

$$+ \frac{\alpha_s\langle G_{\mu\nu}^a G_{\mu\nu}^a\rangle}{12\pi M^4} + \tfrac{208}{81}\pi\alpha_s\frac{\langle\bar{q}q\rangle^2}{M^6}\left\{1 + \tfrac{2}{13}\frac{Q^2}{M^2}\right\} + O\left(\frac{1}{M^8}\right) + O(\alpha_s). \tag{10}$$

For the condensates we use the standard values:

$$\frac{\alpha_s}{\pi}\langle G^a_{\mu\nu}G^a_{\mu\nu}\rangle = 0.012\ \text{GeV}^4, \tag{11}$$

$$\alpha_s\langle\bar{q}q\rangle^2 = 1.8\cdot 10^{-4}\ \text{GeV}^6 \tag{12}$$

obtained in Ref. [9] from the analysis of 2-point functions.

An apparent discrepancy is that the l.h.s. of Eq. (10) has no dependence on M^2 while the r.h.s. of Eq. (10) is a nontrivial function of this parameter. However, if one takes into account all the nonperturbative corrections and uses for $\varrho(s_1, s_2, Q^2)$ an exact rather than model expression, then the r.h.s. of the sum rule (10) also becomes independent of M^2. It is easy to establish that for sufficiently large M^2 our theoretical "prediction" for $f_\pi^2 F_\pi(Q^2)$ has a very weak dependence on the "unphysical" parameter M^2, but the onset of the asymptotic regime strongly depends on s_0 (Fig. 5).

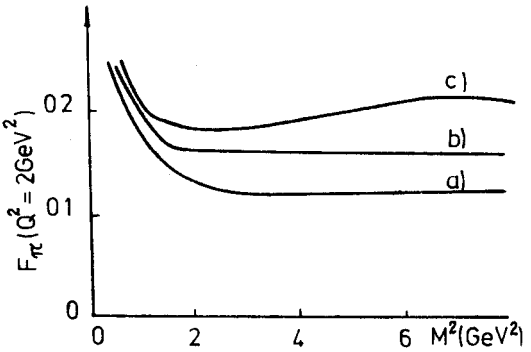

Fig. 5. Typical dependence of the r.h.s. of Eq. (10) on the s_0-parameter. a) $s_0 = 0.6\ \text{GeV}^2$; b) $s_0 = 0.7\ \text{GeV}^2$; c) $s_0 = 0.8\ \text{GeV}^2$; $Q^2 = 2\ \text{GeV}^2$

The true value of s_0 is evidently that for which the region of weak sensitivity to variations of M^2 is the largest one. For $Q^2 = 1, 2, 3\ \text{GeV}^2$ this criterion gives for s_0 values close to $0.7\ \text{GeV}^2$. It should be noted that this is just the value extracted from the analysis of the 2-point function related to $\langle Tj_\beta j_\alpha\rangle$. For $s_0 = 0.7\ \text{GeV}^2$ the combination $f_\pi^2 F_\pi(Q^2)$ is practically constant in the whole region $M^2 \gtrsim 1\ \text{GeV}^2$, and as a final theoretical prediction on $f_\pi^2 F_\pi(Q^2)$ we take its asymptotic value for $M^2 = \infty$.

An important observation is that for $M^2 = \infty$ the power corrections vanish, and one arrives at the finite energy sum rule (cf. [16]):

$$f_\pi^2 F_\pi(Q^2) = \frac{1}{\pi^2}\int_0^{s_0} ds_1 \int_0^{s_0} ds_2 \varrho^{\text{pert}}(s_1, s_2, Q^2), \tag{13}$$

which is just the local duality relation between the resonance (pion) and free-quark contributions. A similar sum rule for the 2-point function gives a simple relation between s_0 and f_π:

$$s_0 = 4\pi^2 f_\pi^2. \tag{14}$$

This relation is in a good agreement (for $s_0 = 0.7\ \text{GeV}^2$) with the experimental value $f_\pi = 132\ \text{MeV}$.

Using the explicit form (6) of $\varrho^{\text{pert}}(s_1, s_2, Q^2)$ one can reduce Eq. (13) to

$$F_\pi(Q^2) = \frac{s_0}{4\pi^2 f_\pi^2}\left\{1 - \frac{1+6s_0/Q^2}{(1+4s_0/Q^2)^{3/2}}\right\}. \tag{15}$$

Note that Eq. (14) provides the correct normalization of $F_\pi(Q^2)$ for $Q^2 = 0$.

Another formula for $F_\pi(Q^2)$ can be obtained if one substitutes integration over the square ($0 \leqslant s_1 \leqslant s_0$; $0 \leqslant s_2 \leqslant s_0$) in Eq. (13) by integration over the triangle ($0 \leqslant s_1 + s_2 \leqslant S_0$) of equivalent area. This gives

$$F_\pi^{(\text{TR})}(Q^2) = \frac{S_0}{8\pi^2 f_\pi^2 (1+Q^2/2S_0)^2} \tag{16}$$

where $S_0 = \sqrt{2}s_0 \simeq 1\ \text{GeV}^2$. For $Q^2 \gtrsim 1\ \text{GeV}^2$ Eq. (16) reproduces Eq. (15) with an accuracy better than 10%.

Eq. (16) corresponds to a dipole behaviour of the pion form factor, in an apparent contradiction with the general prejudice about the behaviour of $F_\pi(Q^2)$. In fact, however, the theoretical curve based on Eq. (15) for $s_0 = 0.7\ \text{GeV}^2$ is in a good agreement with the experimental data (see Fig. 6). Moreover, for $Q^2 \geqslant 1\ \text{GeV}^2$ it coincides with the best fit [17] to the existing data [18].

In other words, Eq. (15) in the region $0.5 \leqslant Q^2 \leqslant 5\ \text{GeV}^2$ imitates the $1/Q^2$ behaviour suggested by the quark counting rules.

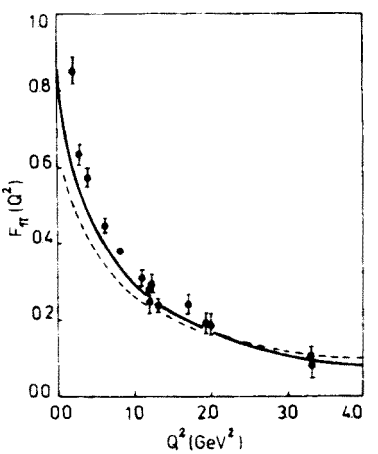

Fig. 6. Comparison of theoretical predictions based on the QCD sum rule (10) with experimental data [18]. Solid line: $M^2 = \infty$, dashed line: $M^2 = 1.8\ \text{GeV}^2$

3. Local quark-hadron duality and the soft pion wave function

Incorporating the local duality ansatz (13) is equivalent to fixing the soft pion wave function (s.w.f.). Indeed, taking into account that $\varrho_i^{\text{pert}}(s_1, s_2, Q^2)$ is the double discontinuity (in p_1^2 and p_2^2) of the amplitude $T_i(p_1^2, p_2^2, Q^2)$, it is easy to realize that the prescription

of Eq. (13) reduces, for Fig. 2, to the substitution s.w.f. $\to \Gamma$, where Γ is a local vertex corresponding to transition of the j-current into free, almost massless quarks, with subsequent averaging of the invariant mass s of the 2-quark system over the region $0 \leqslant s \leqslant s_0$. In other words, the pion is treated as a system composed of 2 on-shell ($k_i^2 = m_q^2$) quarks localized inside a sphere $(k_1 + k_2)^2 \leqslant s_0$ in the momentum space. This picture, in particular, has a merit of being both relativistically and gauge invariant.

It is instructive to observe that in the infinite momentum frame (IMF) such a wave function is proportional to $\theta(\kappa^2 < s_0)$, κ^2 being the usual IMF combination (cf. Ref. [6])

$$\kappa^2 = \sum_{i=1}^{2} \frac{k_{\perp i}^2}{x_i}, \tag{17}$$

where x_i is the IMF fraction of the pion longitudinal momentum carried by the i-th quark, and $k_{\perp i}$ is its transverse momentum. It is also worth comparing the wave function $\varphi^{(\mathrm{LD})} \sim \theta(\kappa^2 < s_0)$, suggested by the local quark-hadron duality, with the Gaussian $\psi^{(\mathrm{G})}(k_\perp, x) \sim \exp(-R^2\kappa^2)$ and power-law $\psi^{(\mathrm{P})}(k_\perp, x) \sim (\kappa^2 + \mu^2)^{-\alpha}$ model wave functions considered by Brodsky and Lepage [19]. All the wave functions have a common property: the cut-off for large κ^2 values. Of course, the sharp cut-off $\kappa^2 \leqslant s_0$ dictated by $\varphi^{(\mathrm{LD})}(k_\perp, x)$ is unrealistic: the exact nucleon s.w.f. should be a smooth function of κ, like $\psi^{(\mathrm{G})}(k_\perp, x)$ or $\psi^{(\mathrm{P})}(k_\perp, x)$.

Thus, $\varphi^{(\mathrm{LD})}(k_\perp, x)$ can reproduce only the most general (i.e., integral) properties of the exact pion soft wave function. Correspondingly, one should not expect that $F_\pi(Q^2)$ calculated according to Eq. (10) must coincide with the exact contribution of the triangle diagram (Fig. 2a) in the whole region $0 < Q^2 < \infty$.

In particular, one should not trust Eq. (10) in the Q^2 regions where its contribution has an essential dependence on the specific behaviour of the s.w.f. at the edges of the kinematically allowed region, when $x_i = 0$ or 1 for some i. As it follows from Eq. (5), the behaviour of Φ^{pert} (and, hence, of ϱ^{pert}) for small Q^2 has an essential dependence on the behaviour of the integrand in the region $x \sim 1$ where a bulk part of the longitudinal IMF momentum of the pion is carried by the passive quark; while for large Q^2 values the dominant contribution to $\varrho(s_1, s_2, Q^2)$ is due to integration over the region $x^{(\mathrm{A})} \sim 1$ where the pion momentum is carried mainly by the active quark. Thus, one should rely on Eq. (10) neither for very small nor for asymptotically large Q^2 values.

A more quantitative estimate of the applicability region of Eq. (10) may be obtained in the following way. Note, first, that the perturbative calculations for the original amplitude $T(p_1^2, p_2^2, Q^2)$ are reliable only within the asymptotic freedom region $Q^2 \gtrsim m_\varrho^2 \sim 0.6\ \mathrm{GeV}^2$. On the other hand, for large Q^2 one should not trust Eq. (10) in the Q^2 region where the asymptotic regime $F_\pi^{(\mathrm{LD})} \sim 1/Q^4$ sets in, because in this case the largest contribution comes from the integration over the region where the off-shellness of the passive quark is $\lesssim p^4/Q^2$, i.e. also beyond the asymptotic freedom domain. It is easy to establish that Eq. (15) agrees (within 50%) with the asymptotic formula $F_\pi^{(\mathrm{LD,as})}(Q^2) \simeq 6s_0^2/Q^4$ only starting from $Q^2 = 7\ \mathrm{GeV}^2$, and just for $Q^2 \gtrsim 7\ \mathrm{GeV}^2$ the product $Q^2 F_\pi^{(\mathrm{LD})}(Q^2)$ becomes a decreasing function of Q^2 (this is also a signal of the onset of the asymptotic regime).

Thus, there exists the intermediate region $0.5 < Q^2 < 5\ \text{GeV}^2$ where the contribution of the triangle diagram is determined just by the integral properties of the s.w.f., mainly by the width of the quark distribution in the transverse momentum (i.e. eventually, by the pion size). The dependence on the specific form of such a distribution in this region is rather weak.

The dimensional parameter that characterizes the width of the $k_\perp$-distribution for $\varphi^{(\mathrm{LD})}(k_\perp, x)$ is clearly s_0 (in fact, $\langle k_\perp^2 \rangle = s_0/10 \approx (300\ \text{MeV})^2$), i.e. the same parameter that sets the scale of the meson mass spectrum in the axial channel. Such a connection seems to be quite reasonable from a physical standpoint.

4. Local quark-hadron duality and nucleon form factors in QCD [15]

The technique described above can be used also to calculate the nucleon EM form factors. Of course, the axial current in Eq. (1) should be substituted by a current having the nucleon quantum numbers, e.g., for the proton one may take [10]:

$$\eta_\alpha = (u^a C^{-1} \gamma_\lambda u^b)(\gamma_5 \gamma^\lambda d^c)_\alpha \varepsilon_{abc}, \tag{18}$$

where C is the charge conjugation matrix, and ε_{abc} is the antisymmetric tensor ($a, b, c = 1, 2, 3$). For the neutron one should interchange $u \leftrightarrow d$ in Eq. (18).

The 3-point amplitude $T^\mu_{\alpha\beta}(p_1, p_2)$ in this case is the sum of structures like $P^\mu \not{P}_{\alpha\beta} \equiv V^\mu_{\alpha\beta}(P)$, $q^\mu \not{P}_{\alpha\beta}$, $q^2 \gamma^\mu_{\alpha\beta}$, $i\varepsilon^{\mu\lambda\sigma\varrho} P_\lambda q_\sigma (\gamma_5\gamma_\varrho)_{\alpha\beta} \equiv A^\mu_{\alpha\beta}(P, q)$ etc. The leading IMF structure is $V^\mu_{\alpha\beta}(P)$. Note that for $p_1^2 = p_2^2$ the $V^\mu_{\alpha\beta}$-structure satisfies the transversality condition $q_\mu V^\mu_{\alpha\beta}(P) = 0$. Another structure possessing this property is $A^\mu_{\alpha\beta}(P, q)$, linear in the "small" parameter q. The corresponding invariant amplitudes will be denoted as T_V and T_A, respectively. It should be emphasized that these two structures have the most direct connection with the $\not{P}_{\alpha\beta}$-component of the 2-point function $\Pi_{\alpha\beta}$ related to $\langle T\eta_\alpha \bar{\eta}_\beta \rangle$. The latter was studied in detail in Ref. [20]. The value of the duality interval s_0 according to Ref. [20] is $s_0 = 2.3\ \text{GeV}^2$. This value will be used in our subsequent analysis. Note also that in the local duality approximation s_0 can be related to the "proton decay constant" λ_N

$$\langle 0|\eta_\alpha|P\rangle = \lambda_N v_\alpha(P) \tag{19}$$

(where $v_\alpha(P)$ is the Dirac spinor) by the formula

$$(2\pi)^4 \lambda_N^2 = s_0^3/12 \tag{20}$$

analogous to Eq. (14).

Computing $\varrho^{\mathrm{pert}}_{V,A}(s_1, s_2, Q^2)$ for the diagram 2a and substituting the results into an analog of Eq. (10) we obtained for the proton

$$F_V^p(Q^2) = \frac{1}{(2\pi)^4 \lambda_N^2} \int_0^{s_0} ds_1 \int_0^{s_0} ds_2 Q^2 \left(1 - \frac{\sigma}{z}\right)^2$$

$$\times \left\{ \frac{2e_u - e_d}{16} \frac{Q^2}{z} \left(1 + \frac{\sigma}{z}\right)^2 + \frac{e_u + e_d}{12} \left(2 + \frac{\sigma}{z}\right) \right\}, \tag{21}$$

$$F_A^p(Q^2) = \frac{e_u}{(2\pi)^4 \lambda_N^2} \int_0^{s_0} ds_1 \int_0^{s_0} ds_2 \frac{Q^2}{4} \left(1 - \frac{\sigma}{z}\right)^2 \left(2 + \frac{\sigma}{z}\right), \tag{22}$$

where $\sigma = s_1 + s_2 + Q^2$, $z = \sqrt{\sigma^2 - 4s_1 s_2}$, $e_u = 2/3$, $e_d = -1/3$. To get the neutron form factors one should interchange $e_u \leftrightarrow e_d$ in Eqs. (21), (22).

To compare Eqs. (21), (22) with experimental data, one should substitute λ_N^2 by its value dictated by Eq. (20) and take $s_0 = 2.3\ \text{GeV}^2$. One should also take into account that $\mathscr{F}_V(Q^2)$ is a combination of the electric G_E and magnetic G_M Sachs form factors

$$\mathscr{F}_V(Q^2) = \frac{4m_N^2 G_E(Q^2) + Q^2 G_M(Q^2)}{Q^2 + 4m_N^2}. \tag{23}$$

For small Q^2 the r.h.s. of Eq. (23) reduces to $G_E(Q^2)$ while for large Q^2 (in fact, for $Q^2 \gtrsim 10\ \text{GeV}^2$) it may be treated as $G_M(Q^2)$. The second form factor $F_A(Q^2)$ coincides with $G_M(Q^2)$.

It is easy to derive that as $Q^2 \to \infty$ the r.h.s. of Eq. (21) tends to that of Eq. (22), and the two expressions give the same result

$$G_M^{p(n)}(Q^2) \sim \frac{4e_{u(d)} s_0^3}{Q^6}$$

for the asymptotic behaviour of the magnetic form factors. It should be emphasized, however, that the asymptotic $O(Q^{-6})$ regime for Eqs. (21) and (22) sets in only for $Q^2 \gtrsim 20$–$30\ \text{GeV}^2$. In fact, the products $Q^4 \mathscr{F}_V(Q^2)$ and $Q^4 G_M(Q^2)$ as predicted by Eqs. (21) and (22) are constant within 10% for Q^2 varying from 5 to 15 GeV^2. In other words, Eqs. (21) and (22) imitate the power law behaviour $G_M \sim 1/Q^4$ dictated by the QCR [1, 2] up to the Q^2-values as large as 20 GeV^2. In higher orders, however, one should take into account also a possible modification of Eqs. (21) and (22) for large Q^2 by the Sudakov form factor of the struck quark:

$$S(Q^2, M^2) = \exp\left\{-\tfrac{8}{27}\left[\ln\frac{Q^2}{\Lambda^2} - \tfrac{3}{2}\right] \ln\frac{\ln Q^2/\Lambda^2}{\ln M^2/\Lambda^2} - \ln\frac{Q^2}{M^2}\right\} \tag{24}$$

where the scale M^2 is proportional to s_0, the only dimensionful parameter in Eqs. (21) and (22). Note that the value of M^2 is rather large whereas the QCD Λ-parameter is presumably small ($\Lambda \sim 100\ \text{MeV}$) and, as a result, in the accessible region $Q^2 \lesssim 20$–$30\ \text{GeV}^2$ the Sudakov suppression of Eqs. (21) and (22) is not very strong. Furthermore, such a suppression may be partly compensated by contributions of the diagrams 2b, c. Thus, it seems quite reasonable to neglect the higher order corrections for $Q^2 \lesssim 20\ \text{GeV}^2$, and expect in this region a good agreement between the local quark-hadron duality predictions and experimental data.

5. Numerical analysis of the local duality results for the nucleon form factors

Now we turn to the comparison of the predictions of Eqs. (21) and (22) with the existing experimental data.

a) Proton form factors. Note first that $G_M^p(Q^2)$ obtained from Eq. (22) in the region $Q^2 = 2$–$10\ \mathrm{GeV}^2$ is in 10% agreement with the empirical dipole fit $G_M^p(Q^2) = \mu_p D(Q^2)$ (where $\mu_p = 2.79$ and $D(Q^2) = (1 + Q^2/0.71)^{-2}$) (see the Table, first line). Furthermore, using Eqs. (21)–(23) one can obtain an explicit expression for $G_E(Q^2)$ and observe that $G_E^p(Q^2) \simeq D(Q^2)$ within 10% for $Q^2 \lesssim 12\ \mathrm{GeV}^2$. (The Table, third line). As a result, the scaling relation $G_M^p(Q^2)/G_E^p(Q^2) \simeq \mu_p$ holds within 15% for Q^2 ranging from 3 to $15\ \mathrm{GeV}^2$. On the other hand, assuming that $G_M^p(Q^2)/G_E^p(Q^2) = \mu_p$ for all Q^2, one can extract $G_M^p(Q^2)$ from Eq. (21) which is presumably more precise for small Q^2 values than Eq. (22)[1]. Indeed,

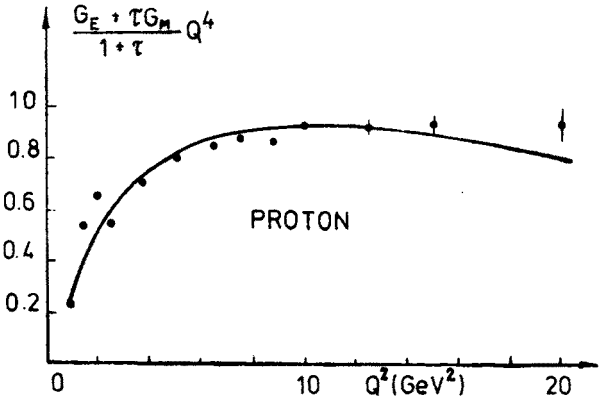

Fig. 7. Proton form factor $Q^4 \mathscr{F}_V(Q^2)$. Data from Ref. [21]

the results for $G_M^p(Q^2)$ obtained in this way are in a better agreement with the dipole fit for $Q^2 = 1$–$2\ \mathrm{GeV}^2$ than those extracted from Eq. (22) (see the Table, second line and Fig. 7).

b) Neutron magnetic form factor. The predictions of Eqs. (21) and (22) for $G_M^n(Q^2)$ agree with the data within the experimental uncertainties only for $Q^2 \gtrsim 6\ \mathrm{GeV}^2$ (Fig. 8). In the region $Q^2 \lesssim 6\ \mathrm{GeV}^2$ the agreement between the neutron version of Eq. (22) and experiment is not so impressive as that for G_M^p. In particular, the prediction of Eq. (22) for the ratio $G_M^n(Q^2)/D(Q^2)$ in the $Q^2 = 3$–$6\ \mathrm{GeV}^2$ region is by 30% lower than that observed experimentally (Table, 4-th line). The disagreement is even more drastic for $Q^2 = 1$–$2\ \mathrm{GeV}^2$. If one calculates $G_M^n(Q^2)$ from Eq. (21) assuming that $G_E^n(Q^2) = 0$, then the disagreement between theory and experiment for $Q^2 = 1$–$4\ \mathrm{GeV}^2$ is reduced, but only to 20% (Table, 5-th line). The situation may be interpreted so that the difference between the exact nucleon

[1] Note that the structure $V_{\alpha\beta}^{\mu}$ relevant to Eq. (21) has no damping for small q; hence, for small Q^2 the original amplitude $T_{\alpha\beta}^{\mu}(p_1, p_2)$ is more sensitive to the contribution of T_V than to that of T_A.

TABLE

Numerical results based on Eqs. (21)–(23)

	$Q^2(\mathrm{GeV}^2)$	1	2	3	4	5	6	8	10	12	15	20	30
1	$G_M^p(Q^2)/\mu_p D(Q^2)$	0.79	0.93	1.00	1.02	1.03	1.01	0.97	0.92	0.86	0.79	0.68	0.53
2	$G_M^p(Q^2)/\mu_p D(Q^2)$	0.91	1.01	1.05	1.05	1.04	1.02	0.97	0.91	0.86	0.78	0.67	0.53
3	$G_E^p(Q^2)/D(Q^2)$	1.00	1.13	1.16	1.15	1.11	1.06	0.95	0.86	0.77	0.67	0.54	0.38
4	$G_M^n(Q^2)/\mu_n D(Q^2)$	0.58	0.58	0.73	0.75	0.75	0.74	0.71	0.67	0.63	0.58	0.50	0.39
5	$G_M^n(Q^2)/\mu_n D(Q^2)$	0.82	0.80	0.79	0.77	0.76	0.74	0.70	0.65	0.61	0.56	0.49	0.38
6	$G_E^n(Q^2)/D(Q^2)$	−0.13	−0.12	−0.10	−0.06	−0.03	0.00	0.05	0.08	0.11	0.13	0.14	0.14
7	$M_N(\mathrm{GeV})$	0.74	0.83	0.87	0.90	0.92	0.94	0.97	0.98	1.00	1.01	1.02	1.04

w.f. and that suggested by the quark-hadron duality is more essential for $G_M^n(Q^2)$ than for $G_M^p(Q^2)$. It is worth emphasizing here that such a proton-neutron asymmetry does not contradict the isotopic invariance. In particular, studying the power corrections in the (exponential-weighted) QCD sum rules for $G_M(Q^2)$, we have observed that for the proton the most essential $\langle\bar{q}q\rangle^2$ corrections are proportional to e_d, while the ground term according to Eq. (22) is proportional to e_u. As a result, the ratio of the $\langle\bar{q}q\rangle^2$ correction to the ground term for the neutron is 4 times as large as that for the proton.

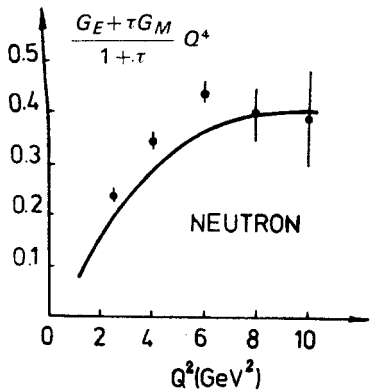

Fig. 8. Neutron form factor $Q^4\mathcal{F}_V(Q^2)$

c) Neutron electric form factor and the nucleon mass estimate. Using Eqs. (21)–(23) one can calculate $G_E^n(Q^2)$ and observe that the predicted $G_E^n(Q^2)$ values are very close to zero for $Q^2 = 2$–20 GeV^2. (Table, 6-th line). It should be stressed here that the smallness of $G_E^n(Q^2)$ reflects a nontrivial correlation between the values of $F_V^n(Q^2)$, $G_M^n(Q^2)$ predicted by Eqs. (21) and (22) and the magnitude of the nucleon mass parameter m_N^2 entering into Eq. (23). For instance, requiring $G_E(Q^2)$ to be exactly zero, one can extract the nucleon mass from Eqs. (21)–(23). In the region $Q^2 = 2$–30 GeV^2 such a procedure gives for m_N the values very close to the experimental ones (Table, 7-th line).

d) Ratio $G_M^p(Q^2)/G_M^n(Q^2)$. According to Eq. (22), the ratio $G_M^p(Q^2)/G_M^n(Q^2)$ equals (-2) for all Q^2. In its turn, Eq. (21) (combined with the assumption that $G_E(Q^2)/G_M(Q^2) = G_E(0)/G_M(0)$) predicts that $|G_M^p(Q^2)/G_M^n(Q^2)|$ is smaller than 2 for $Q^2 \lesssim 4$ GeV^2 (e.g. 1.6 for $Q^2 = 1$ GeV^2), but in the region $Q^2 \gtrsim 4$ GeV^2 Eq. (21) also gives $G_M^p(Q^2)/G_M^n(Q^2) = -2$. This prediction agrees well with the recent data [21] in the $Q^2 \gtrsim 6$ GeV^2 region.

e) Magnetic moments. As emphasized earlier, there are no grounds to expect Eq. (22) to agree with the experimental data in the region $Q^2 \lesssim 1$ GeV^2. However, the values of magnetic moments $\mu_p \equiv G_M^p(0) = 4e_u = 8/3$ and $\mu_n \equiv G_M^n(0) = 4e_d = -4/3$ predicted by Eq. (22) are in satisfactory agreement with the experimental ones ($\mu_p^{exp} = 2.79$; $\mu_n^{exp} = -1.91$). Note that just as it was for $Q^2 \gtrsim 1$ GeV^2, the model is more successful for the proton than for the neutron. It is intriguing to observe also that the ratio $(|\mu_n| - 4/3)/(\mu_p - 8/3)$ is indeed close to 4.

5. Conclusions

Thus, in a rather wide region $Q^2 = 2$–$15\ \mathrm{GeV}^2$ the nucleon form factors calculated according to the local quark-hadron duality prescription are in satisfactory (or even good) agreement with the experimental data. One of the most nontrivial results here is that the ratio $G_M^p(Q^2)/G_M^n(Q^2)$ for sufficiently large Q^2 is predicted by Eqs. (21) and (22) to take just the value (-2) suggested by the recent experimental data [21]. For the pion form factor we observed a good agreement between the theoretical calculations and the experimental results in the region $0.5 < Q^2 < 5\ \mathrm{GeV}^2$. Both for the nucleons and for the pion the good description of the data was obtained within the lowest (zero) order approximation in α_s, without including numerically suppressed by $\alpha_s/\pi \sim 0.1$ and $(\alpha_s(\pi))^2 \sim 0.01$ contributions due to the diagrams containing gluon exchanges. We observed also that the theoretically calculated behaviour of the form factors in these Q^2-regions has an essential dependence on the parameters (of s_0 type) characterizing the size of the hadron considered. The formulas obtained have a rather complicated dependence on Q^2 and s_0 which imitates for moderately large Q^2 the simple power behaviour $F_\pi(Q^2) \sim 1/Q^2$, $G_{M,E}^N(Q^2) \sim 1/Q^4$ suggested by the quark counting rules [1, 2].

It should be emphasized, however, that the main contribution to the form factors in this Q^2-region comes from integration over the virtual momenta k with $|k^2|$ smaller or of an order of the scale s_0. Evidently, in such a situation there is no justification to use approximations (like scale invariance, say) based on smallness of the ratio $s_0/|k^2|$. Hence, the experimentally observed power-law fall-off of the nucleon form factors reflects only the finite size of the hadrons rather than the approximate short-distance scale invariance of the underlying field theory. In other words, the observed dipole behaviour of the proton magnetic form factor, e.g., has nothing to do with two-gluon-exchange diagrams of Fig. 1. The latter come into play and dominate only for very large Q^2, when the contributions of the simplest $O(\alpha_s^0)$ diagrams will be sufficiently damped, say, by the Sudakov form factor of the active quark. Only for very large Q^2 (probably, far beyond all experimental possibilities) the short-distance dynamics is responsible for the behaviour of the hadronic form factors and only then it makes sense to use the asymptotic analysis developed in Refs. [1–8].

All these remarks are true also for many other exclusive processes, e.g., for the wide-angle scattering of the hadrons, and for the behaviour of hadronic structure functions for $x \sim 1$. In all cases, when the diagrams containing no gluon exchanges are not forbidden (say, by conservation laws), just these diagrams should be taken into account in the first place. There is no need, for instance, to waste efforts and time for calculating millions of $O(\alpha_s^5)$ diagrams responsible for (astronomically distant) asymptotics of the pp wide-angle scattering amplitude.

I thank V. A. Nesterenko for help in calculations and many stimulating discussions. I am most grateful to A. Białas, K. Zalewski and M. Praszałowicz for kind hospitality in Zakopane.

REFERENCES

[1] V. A. Matveev, R. M. Muradyan, A. N. Tavkhelidze, *Lett. Nuovo Cimento* **7**, 719 (1973).
[2] S. J. Brodsky, G. R. Farrar, *Phys. Rev. Lett.* **31**, 1153 (1973).
[3] A. V. Radyushkin, JINR Preprint P2-10717, Dubna 1977.
[4] S. J. Brodsky, G. P. Lepage, Preprint SLAC-Pub. 2294, Stanford 1979.
[5] A. V. Efremov, A. V. Radyushkin, *Phys. Lett.* **94B**, 245 (1980).
[6] S. J. Brodsky, G. P. Lepage, *Phys. Rev.* **D22**, 2157 (1980).
[7] V. L. Chernyak, Proc. XV LINP Winter School, vol. 1, p. 65, Leningrad 1980 (in Russian).
[8] A. H. Mueller, *Phys. Rep.* **73**, 237 (1981).
[9] M. A. Shifman, A. I. Vainshtein, V. I. Zakharov, *Nucl. Phys.* **B147**, 385, 447 (1979).
[10] B. L. Ioffe, *Nucl. Phys.* **B188**, 317 (1981).
[11] V. A. Nesterenko, A. V. Radyushkin, *JETP Lett.* **35**, 488 (1982).
[12] V. A. Nesterenko, A. V. Radyushkin, *Phys. Lett.* **115B**, 410 (1982).
[13] B. L. Ioffe, A. V. Smilga, *Phys. Lett.* **114B**, 353 (1982); *Nucl. Phys.* **B216**, 373 (1983).
[14] V. A. Nesterenko, A. V. Radyushkin, *Yad. Fiz.* **38**, 476 (1983).
[15] V. A. Nesterenko, A. V. Radyushkin, *Phys. Lett.* **128B**, 439 (1983); *Yad. Fiz.* **39**, 1287 (1984).
[16] N. V. Krasnikov, A. A. Pivovarov, *Phys. Lett.* **112B**, 397 (1982).
[17] C. A. Dominguez, *Phys. Rev.* **D25**, 3084 (1982).
[18] C. Bebek et al., *Phys. Rev.* **D17**, 1693 (1978).
[19] S. J. Brodsky, G. P. Lepage, Preprint SLAC-Pub. 2605, Stanford 1980.
[20] V. M. Belyaev, B. L. Ioffe, *Zh. Eksp. Teor. Fiz.* **93**, 876 (1982); V. M. Belyaev, *Phys. Lett.* **127B**, 254 (1983).
[21] S. Rock et al., SLAC-Pub. 2449, Stanford 1982.